Minimal Communication between Drones Using Guidance Vector Fields in Dense Airspace

1st Adrian del Ser
ENAC Drones and UTM Chair
ENAC, Université de Toulouse
Toulouse, France
adrian.del-ser@enac.fr

2nd Murat Bronz
Dynamic Systems, OPTIM
ENAC, Université de Toulouse
Toulouse, France
murat.bronz@enac.fr

***Abstract*—In response to escalating drone traffic, this paper investigates the interplay between drone density, communication frequency, and collision avoidance. We utilize artificial potential fields as a guidance mechanism for drones navigating in dense airspace. Through numerical simulations involving two to nine drones, we analyze how communication frequency correlates with collision rates as drone density increases. Our findings reveal the nuanced relationship between these variables, showing that communication frequency requirements increase with drone density for collision-free navigation. Furthermore, we present a theoretical framework predicting the relationship between drone density and the minimal communication frequency required for safe operations. We also demonstrate a simple experiment in the flying arena to highlight the influence of the rate of positional information sharing on the paths taken by drones.**

***Index Terms*—Artificial Potential Fields, communication frequency, collision avoidance**

I. Introduction

Unmanned aerial vehicles (UAVs), are becoming an increasingly commonplace technology with a wide range of applications spanning logistics, surveillance, agriculture, and beyond. The burgeoning growth in the use of drones is leading to denser aerial environments, which pose significant operational challenges, notably collision avoidance.

Ensuring safe, collision-free drone navigation necessitates robust communication between drones. This communication allows drones to 'perceive' each other in the airspace and adjust their movements accordingly. However, the ideal frequency of this communication remains an area of critical investigation. Too high a frequency can overburden the communication systems and increase power consumption, while too low a frequency can risk late detection of nearby drones, leading to potential collisions.

Many algorithms exist in the field of path planning (for UAVs, ground robots and others), such as the the A* algorithm [1], [2] [3], the rapid exploration random tree (RRT) [4] [5] and artificial potential fields (APF) [6]. APFs are particularly popular in real time applications due to their simplicity and low computational requirement. APF algorithms have been improved continuously, such as adapting the original algorithm used for ground robots to work with quad-rotors [7], tackling the problem of vehicles getting stuck in local minima [8], reducing sharp turn angles as well as energy consumption [9]. [10] combined APF with vortex panel methods (commonly used in airfoil aerodynamic calculations [11]) to allow for the placement and avoidance of obstacles.

The aforementioned path planning works usually assume all attributes such as positions, velocities, altitudes etc. are known at all times. In reality, especially for large swarms of vehicles, maintaining a constant flow of such data necessitates robust inter-vehicle communication [12], [13]. Moreover, for such vast swarms, communication latency could undermine the effectiveness of the deconfliction algorithms. Strategies to mitigate this include clustering vehicles to reduce latency [14] and leveraging cellular 5G networks for reliable communications [15].

In the quest to optimize these strategies, the need for prudent use of bandwidth often emerges as an important consideration [16]. This paper takes a deliberate step back to examine the fundamental requirements of inter-drone communication frequency to avoid collisions. By doing so, we aim to identify the minimum frequency required for collision-free operation, thereby contributing to the efficient use of communication resources in large drone swarms.

This study aims to explore the relationship between the rate of inter-drone communication and collision occurrences in dense airspace. We employ a simulation approach, generating a series of pseudo-random cases with an increasing number of drones. We use APF as the path planning and collision avoidance mechanism. The communication frequency is systematically manipulated to study its impact on collision rates. We hypothesise that few collisions will occur until a critical frequency, after which the success rate will drop before flattening out again. We then present a theoretical framework aimed at predicting the minimum communication frequency necessary for safe drone operation. We also investigate a case with two drones both in simulation and in a real experiment inside ENAC's indoor flight arena, Voliere Drones Toulouse Occitanie (VTO). We compare the flight paths generated in simulation and in reality to validate our simulation parameters.

The contributions of this paper are identifying a relationship in 2D numerical simulations between the maximum number of timesteps between positional updates (or positional update

This work has been funded by the ENAC Drones and UTM Research Chair via ENAC Foundation sponsors Airbus and SopraSteria.

frequency) and the number of drones in a fixed area. This relationship is backed up through a theoretical model.

II. Simulation Setup

A. Problem Statement

We investigate the effect of changing the communication rate between drones on the rate of collision in a simulated environment.

The drones are confined to a two-dimensional square arena of side-length 8m. An individual simulation consists of running a case, consisting of N_d drones placed within the arena with specified initial positions and destinations. Each case represents a unique configuration of drone numbers, starting positions, destinations, and communication frequencies. As a path planning algorithm (guiding each drone to its destination while avoiding other drones) we employ APF. By analysing these simulations, we collect statistical data to quantify the impact of communication rate and drone density on collision rates. In the following sections, we delve into the specifics of our case setup, the path planning algorithm, and other parameters that play important roles in our investigation.

B. Case Generation

Simulations were designed to model a variety of scenarios involving different numbers of drones and communication frequencies. For each of 2 through 9 drones, we generated 1000 pseudo-random cases (for 8000 cases in total), with each case specifying the starting positions of the drones and their destinations. Starting positions were at least one collision distance (see Section II-D and Table I) apart to ensure no two drones were colliding at the start of a simulation. One of the scenarios with three drones is shown in Figure 1 to serve as a visual example.

C. Simulating Communication Between Drones

Each case is run with communication rates ranging from updates at every simulation timestep to no communication at all. In our simulation model, each drone is assigned a 'transmitting' boolean attribute. This attribute is set to True if the drone shares its position at the current simulation timestep, and False otherwise. When the 'transmitting' attribute is False for any drone, its peers use the drone's last known location for path planning. It is worth mentioning that the current location of a non-transmitting drone could be predicted more accurately by taking into account its last known velocity and direction. However, this addition would involve an increase in computation time, and it is a subject left for future studies, along with other aspects of communication modeling such as bandwidth saturation, distance effects, communication channel frequency, and external factors.

In our model, as defined in Table I, we set $\Delta t = 0.02\text{s}$, which corresponds to a baseline simulation frequency of 50Hz. To establish a communication frequency of 25Hz, the drones are programmed to communicate every $2\Delta t$; for a frequency of 5Hz, communication occurs every $10\Delta t$, and so on. The path planning process is assumed to occur onboard each drone at the maximum frequency of 50Hz. It is noteworthy that at the start of the simulation, i.e., $t = 0$, all drones are in the transmitting state.

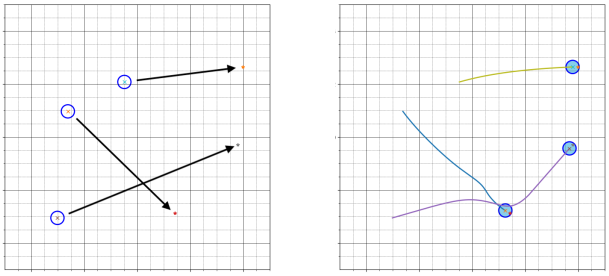

(a) Start (b) End

Fig. 1: Scenario with three drones (with pseudo-random starting and destination positions) at the start and end of a simulation. The path followed by each drone is shown in (b). A circle of radius $r_c/2$ (see Table I) surrounds each drone, if two such circles come into contact (i.e. two drones get to within one collision distance of each other), a collision is recorded.

D. Mathematical Background of Artificial Potential Fields

Drone movements in our study were guided by APFs, a method that has shown promising results in both simulation and in experiments in the VTO flight arena [10].

In the context of this work, APFs were used to model the interactions between individual drones and their environment. Specifically, each drone's destination was modelled as an attractive sink term, while other drones were treated as repulsive sources, each also possessing a vortex term. This vortex term facilitates smooth and predictable trajectory adjustments when drones converge. It ensures a consistent avoidance direction, mirroring the strategies enforced by aviation legislation [17]: for example, a counter-clockwise vortex will prompt both drones to turn right to avoid collision. At each time step, each drone calculates the aggregate effect of its sink, the sources and vortices of other drones, resulting in a vector dictating its movement direction. This vector, updated every Δt, guides the drone's motion along its path. Another way to conceptualise APFs is to envision the instantaneous vector field produced by the sources, vortices, and sink. Each drone moves along the streamline at its location for a duration of Δt. At every new timestep, this streamline changes due to the movements of other drones, leading the drone to follow the updated streamline until the next update occurs. Refer to Figure 2 for a graphical representation of an instantaneous vector field during a simulation.

E. Simulation Parameters

Several parameters are required for the simulations; their values are presented in Table I. The collision distance represents the distance between the centers of two drones, below which a collision is considered to have occurred. The minimum detection distance defines the radius of perception around a drone, beyond which it no longer detects or avoids other

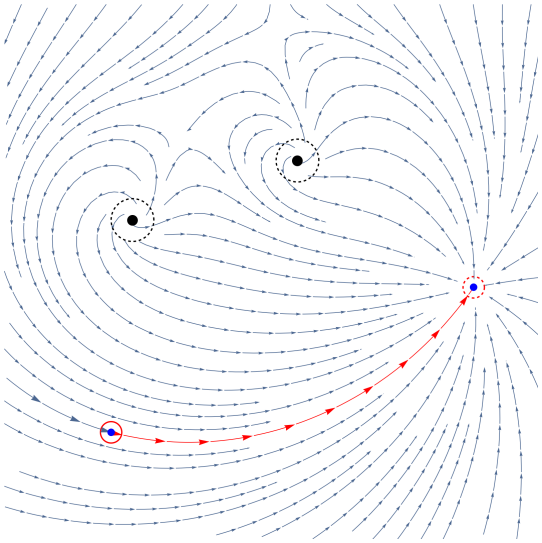

Fig. 2: Instantaneous vector field at $t = 0$ from the perspective of one of three drones, showing its initial path to its destination sink. This path is updated at every time step to account for the movement of other drones, leading to the final path seen in Figure 1 (b).

drones. This concept is particularly valuable for scalability, as it restricts the knowledge of drones about one another to within this radius (see Figure 3 for a visualisation). By detecting drones only a certain distance away, we ensure the computing cost scales with drone density rather than number of drones (assuming guidance calculations using APFs occur onboard each drone). The maximum simulation duration is the maximum time the simulation is allowed to run before starting the next.

By definition, APFs do not take the inertia of drones into account, which inevitably omits real-world constraints imposed by drone momentum. In reality, a drone cannot instantaneously alter its trajectory due to inherent inertia. To accommodate this in our model, we utilize a collision distance r_c, below which any two drones are considered to be colliding. While r_c designates the threshold for conflict, it can also implicitly provide a safety buffer. By adjusting the r_c value appropriately, we can indirectly account for the effect of inertia. A larger r_c allows drones more time and space to enact evasive maneuvers given their inertia. Consequently, while our model assumes zero inertia for simplicity, through the careful selection of the r_c value, we can accommodate the implications of actual drone inertia on collision avoidance.

We acknowledge that there is room for further optimization of these parameters, which were chosen through testing both in numerical simulation (Sec.III) and in the flying arena (Sec.V). Future work could involve the use of reinforcement learning or other data-driven techniques to fine-tune these parameters, resulting in a reduction the distance travelled by the UAVs (and therefore in energy consumption), as well as the likelihood of conflict.

A modification was introduced to the conventional equation

Parameter	Symbol	Value	Units
Square Arena Sidelength	L	8	m
Sink (Goal) Strength	Q_g	5	m^2/s
Source Strength	Q_s	1	m^2/s
Vortex Strength	Q_v	0.25	m^2/s
Drone Velocity	v_d	1	$\mathrm{m\,s}^{-1}$
Collision Distance	r_c	0.5	m
Minimum Detection Distance	r_{det}	2	m
Time Step Size	Δt	0.02	s
Maximum Simulation Duration	-	40	s
Timesteps between updates	n	variable	-
Communication frequency	$f_c(1/n\Delta t)$	variable	s^{-1}
Number of drones	N_d	variable	-

TABLE I: Simulation parameters

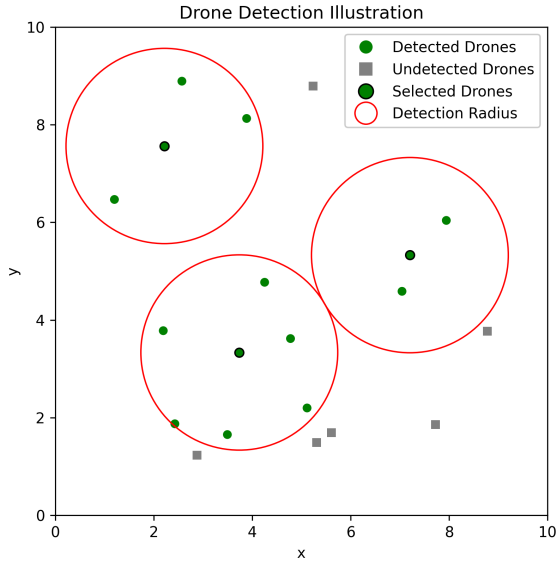

Fig. 3: Illustration to show minimum detection distance. Any drones outside the detection radius of a drone will not be included in its path planning calculation

for velocity induced by a source. The source was modeled to decay with the inverse cube of the distance, rather than the inverse of the distance itself. This adjustment enhances the effect of the source at close range while reducing its influence more rapidly at longer distances (see Figure 4). The revised expressions for the source-induced velocity are as follows:

$$\vec{\mathbf{V}}_{\text{source}} = \frac{Q}{2\pi r}\hat{\mathbf{e}}_{\mathbf{r}} \qquad \text{(Original)} \qquad (1)$$

$$\vec{\mathbf{V}}_{\text{source}} = \frac{Q}{2\pi r^3}\hat{\mathbf{e}}_{\mathbf{r}} \qquad \text{(Modified)} \qquad (2)$$

In these equations, V_{source} represents the velocity induced by the source, Q is a parameter representing the source strength, and r denotes the distance from the source.

III. Results

We have tested 8000 pseudo-randomly generated scenarios using the parameters outlined in Section II-E. Each scenario

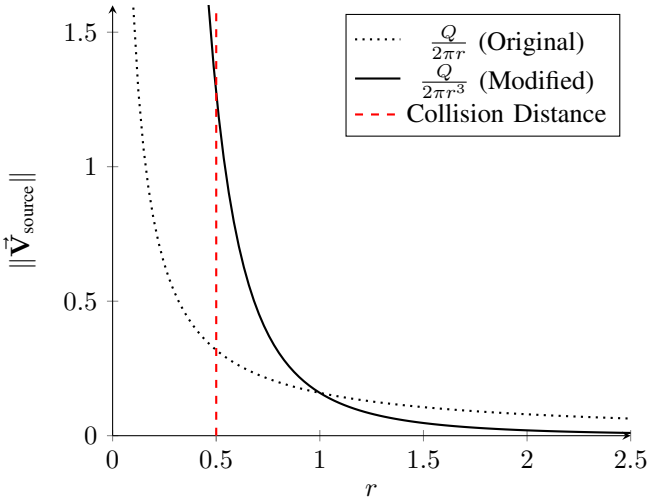

Fig. 4: A comparison illustrating the decay of source-induced velocities with distance for the original and modified formulations.

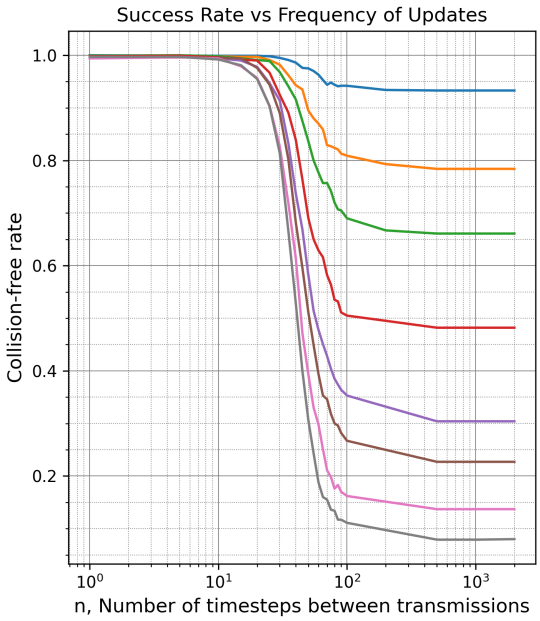

Fig. 5: Numerical Simulation Results. Collision-free rate versus the number of timesteps between position transmissions n, representing decreasing communication frequency. The collision-free rate is calculated as a proportion of 1000 simulations. The x-axis represents the timesteps between updates on a logarithmic scale, ensuring, for example, that halving the frequency is uniformly represented throughout the graph.

simulation was terminated as soon as a collision was detected, marking the scenario as a failure. Out of every 1000 specific simulations with varying drone numbers and frequencies, we noted the number of failures. The results from these simulations, encompassing drone numbers from two to nine, are shown in Figure 5.

The data from the simulations shows a clear correlation between communication frequency and collision rates. This relationship is as we initially hypothesized: with frequencies below a certain threshold, the collision rates remain low. Within the scope of our tested drone numbers, maintaining a communication frequency of at least every $10^1\Delta t$ (or 5Hz) significantly mitigates collision risk. However, it should be noted that these values are dependent on the velocity of the drones - for instance, doubling drone velocity would theoretically necessitate a shift of the curves in Figure 5 towards the left, implying a higher necessary communication frequency.

Furthermore, our simulations suggest that drone numbers play a crucial role in determining the successful operation threshold. For fewer drones, this drop-off in success rate becomes apparent at lower frequencies. For instance, in a scenario with only two drones, the onset of this decline in success rate occurs around $n \approx 25$, compared to $n \approx 10$ for scenarios with nine drones. This shift towards lower frequencies implies that, as drone numbers increase, the requisite communication frequency for successful operation also increases.

These findings form the basis for our theoretical exploration in Section IV, where we endeavor to further interpret these results. Through this, we aim to provide a comprehensive model to predict behavior under varying drone velocities and numbers, contributing towards improved scalability and efficiency in drone operation.

IV. Theoretical Framework

We propose a simplified theoretical model to estimate how the minimum frequency of communication required to avoid drone collisions scales with drone density and velocity. We then combine the observed results from Figure 5 with this model to predict the minimum frequency for higher drone counts.

A. Analysis of Simplified Collision Model

The first step in this model is to predict how a collision occurs. We take the worst case scenario where two drones at $t = t_0$ are heading directly towards each other at a closing speed of $2v$ as depicted in Figure 6.

The initial distance separating the drones is $d_0 + r_c$ (i.e. one drone is at a distance d_0 from entering the collision radius r_c of the other). We assume that if the drones communicate their position at any point after this, then they are able to avoid each other with evasive manoeuvres thanks to the highly repulsive source terms which grow rapidly as distance between drones reduces (see Figure 4). As a consequence, we assume that the last communication occurs at $t = t_0$, and that the collision will occur at $t = t_0 + n\Delta t$, where the communication frequency $f_{c,\text{min}} = 1/(n\Delta t)$ (i.e. the drones would have had their next opportunity to communicate at the moment of collision, thus $f_{c,\text{min}}$ is the minimum required communication frequency to avoid the collision). It follows that

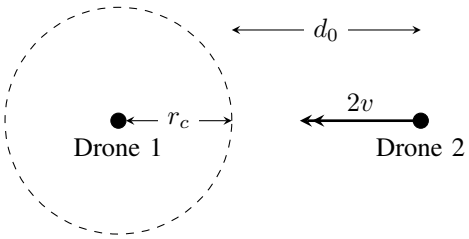

Fig. 6: Illustration of worst case collision scenario. The frame of reference is Drone 1, with Drone 2 approaching at a closing speed of $2v$. The two drones are separated by a distance $r_c + d_0$. Here, r_c denotes the collision radius around Drone 1 (indicated by the dashed circle) and d_0 is the additional separation distance. Drone 2 is thus positioned d_0 units away from Drone 1's collision region.

$$d_0 = 2v(n\Delta t)$$
$$\therefore n = \frac{d_0}{2v\Delta t} \tag{3}$$

and by consequence (since $f_c \geq f_{c,\min}$)

$$f_{c,\min} = \frac{1}{n\Delta t} = \left(\frac{d_0}{2v\Delta t}\Delta t\right)^{-1}$$
$$\therefore f_c \geq \frac{2v}{d_0} \tag{4}$$
$$\text{and } n \leq \frac{d_0}{2v\Delta t} = n_{\max} \tag{5}$$

We are left with a relationship which suggests that the minimum communication frequency to avoid collision is proportional to velocity of the drones and inversely proportional to the distance d_0, which still needs to be predicted.

B. Relationship between Drone Number and Nearest Neighbor Distance

Statistically, we can think of $d_0 + r_c$ as being the average distance between drones before they collide. We also assume that the two drones which collide are each others' nearest neighbors at $t = t_0$. Using these assumptions we need to find the average distance between a drone and its nearest neighbor in our square arena. Even if this prediction for d_0 is not very accurate due to an oversimplified model, the way d_0 scales with number of drones N_d can be used to predict behaviour with higher drone densities. For two drones, which are necessarily each others' nearest neighbors, the nearest neighbor distance is the average distance between two randomly placed points in a square of sidelength L. From [18] this can be analytically expressed as:

$$d_0 + r_c = (2 + \sqrt{2} + 5\ln(\sqrt{2}+1))L/15 \approx 0.52L \tag{6}$$

Plugging in this value for d_0 into (5) and using the values for v, L, r_c and Δt defined in Table I, we obtain $n \approx 92$. This is higher than observed value of $n \approx 25$. Our model may have been too simplistic (specifically, while drones will most likely collide with their nearest neighbor at the last point of communication, most collisions occur when drones get closer than the average nearest neighbor distance), nevertheless we will pursue this approach to find a scaling relationship between d_0 and the number of drones (or the drone density). Assume that the arena initially has just $N_d = 2$ drones with nearest neighbor distance d_0. We increase the number of drones to $N_d = 8$ by splitting the arena into four equal squares with half the sidelength of the original and place two drones into each smaller square. Consequently, we can expect the average nearest neighbor distance halve as well. We deduce therefore that, for a fixed arena size:

$$d_0 \sim 1/\sqrt{N_d} \tag{7}$$

The scaling relationship in (7) can also be estimated by looking at an analysis from [19], pictured in Figure 7.

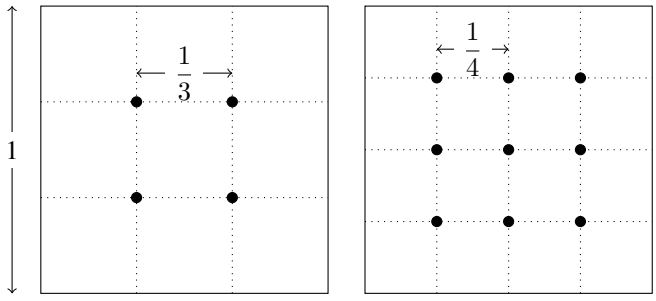

Fig. 7: Simplified formulation to show how distance to nearest neighbor varies with number of drones in a square of unit area [19]. Each black circle represents a drone. By extending the pattern with a greater number of drones N_d, we can deduce that nearest distance between neighbors $d_0 = 1/(\sqrt{N_d}+1)$ which supports our result in (7).

Combining (7) with (5) and (4) we have

$$n_{\max} \sim N_d^{-1/2} v^{-1} \Delta t^{-1} \tag{8}$$
$$f_{c,\min} \sim N_d^{1/2} v \tag{9}$$

If the arena area is not fixed, then the scaling relationship follows drone number per unit area (drone density) instead of drone number. For a three dimensional case, the scaling would go as follows: $d_0 \sim N_d^{-1/3}$.

C. Comparison of Simulation Results and Theory

In an attempt to verify scaling relations derived in Section IV in our simulations, we isolate the cases for $N_d = 2$ and $N_d = 8$ as shown in Figure 8. For $N_d = 2$, $n_{\max,2} \approx 25$ and for $N_d = 8$, $n_{\max,8} \approx 10$. Using (8), we expect

$$\left(\frac{n_{\max,2}}{n_{\max,\ 8}}\right)_{\text{theory}} = \left(\frac{N_d = 2}{N_d = 8}\right)^{-\frac{1}{2}} = 2 \tag{10}$$

From our simulations, the actual value observed is $25/10 = 2.5$, compared to the theoretical value of 2. Given the approximate nature of the values for $n_{\max}$ taken from Figure 8, this is

encouraging. In order to verify the scaling hypotheses from (8) and (9) more thoroughly, a lower value of Δt could be used to increase the resolution of the results. A higher number of cases (10,000 instead of 1000 for example) would also be beneficial.

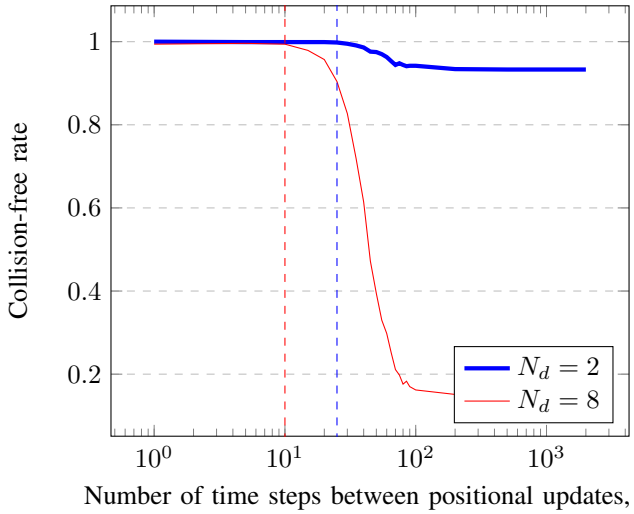

Fig. 8: Collision-free rate versus n (time steps between updates) for 2 and 8 drones. The two vertical lines represent the approximate transition away from collision-free cases ($n_{\max}$)

In order to more thoroughly compare the theoretical and simulated relationship between $n_{\max}$ and N_d, we need a consistent method of deducing $n_{\max}$ from simulated results. It is difficult to deduce from Figure 5 the exact moment at which the collision-free rate drops below 100% (or 1). As a compromise, we propose the following definition: $n_{\max}$ is the number of time-steps between positional updates for which at least 99% of simulations complete without any collisions. We apply this definition (interpolating linearly between the discrete results where necessary) to obtain a value of $n_{\max}$ for each of 2 through 9 drones, plotted on Figure 9. We overlap our result in (8): $n_{\max} = k/\sqrt{N_d}$. The value of k is determined by a least-squares fit to the numerical simulation data.

V. Comparison to Real Flights in the Voliere

A. Experimental Setup

The Voliere is an indoor drone test facility located in Toulouse, France. It contains a usable region of 8m×8m×8m to carry out test flights as shown in Figure 10a.

The test environment is equipped with high-precision localization and measuring instruments, including a state-of-the-art Opti-Track system with 16 cameras operating at 320Hz. The setup allows for the deployment of various types of vehicles for different experiments. As an example, Figure 12b showcases the DJI-Tello quad-rotor, a candidate for use in hardware experiments. This quad-rotor is equipped with a 2.4 GHz 802.11n Wi-Fi connection, enabling control via a ground station. The DJI-Tello model is useful in that it accepts direct input for desired velocity. It strives to adhere to the provided reference velocity by drawing comparisons to its onboard velocity estimation, derived from a downward-facing optic-flow camera.

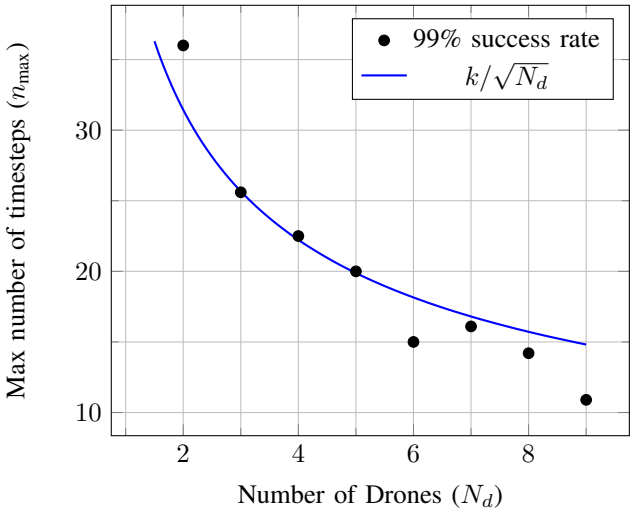

Fig. 9: Numerical simulation versus theoretical relationship between maximum number of time steps between positional updates to ensure a 99% rate of collision-free simulations and the number of drones.

(a) The Toulouse Occitanie Drone Flight Arena (or Voliere)

(b) Tello EDU Quad-rotor

Fig. 10: Images showing the Voliere and quad-rotor used for drone experiments.

B. Trajectory Plots

In an attempt to validate the guidance algorithm used in simulation, we compare one case in simulation with an identical case in experiment. The result is plotted in Figure 11. In Figure 12, we show the effect on the path flown by drones as a result of increasing the number of time steps between positional updates n, both in simulation and in experiment.

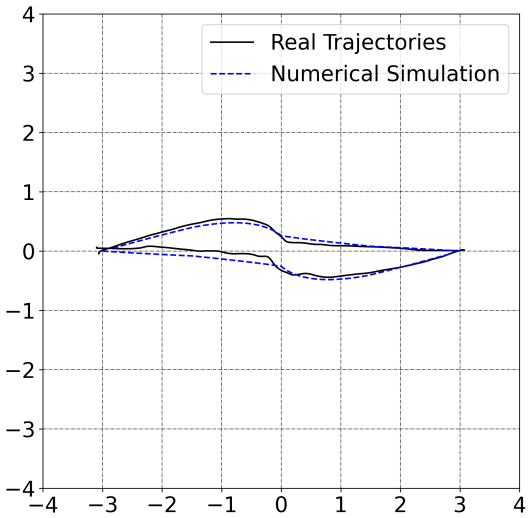

Fig. 11: Visualisation of the paths generated by two drones swapping positions. One drone starts at (-3,0) and flies to (3,0); the other at (3,0) and flies to (-3,0). The dotted line represents the paths taken in the numerical simulation, while the solid line shows the paths taken by real drones in the flying arena. The simulation parameters are $\Delta t = 0.025$s, $n = 120$ (updating positions every 3s), and drone velocity $v_d = 0.5\text{ms}^{-1}$

VI. Conclusions

In this study, we conducted numerical simulations with $N_d = 2$ to $N_d = 9$ drones operating in a defined flying arena to investigate the influence of the number of timesteps between positional updates (n) and identify a threshold, $n_{\max}$, signifying the transition away from fully collision-free operations.

The main findings and contributions related to our research objective can be summarized as follows:

- For each value of N_d, we successfully identified the corresponding threshold value $n_{\max}$. Notably, as the number of drones N_d increased, the required $n_{\max}$ decreased, indicating the necessity for higher update frequencies to maintain collision-free operation with an increasing number of drones.
- A theoretical framework was developed to delve deeper into the relationship between the number of drones and the transition point $n_{\max}$. This framework concluded that in 2D, $n_{\max}$ should scale with $1/\sqrt{N_d}$.

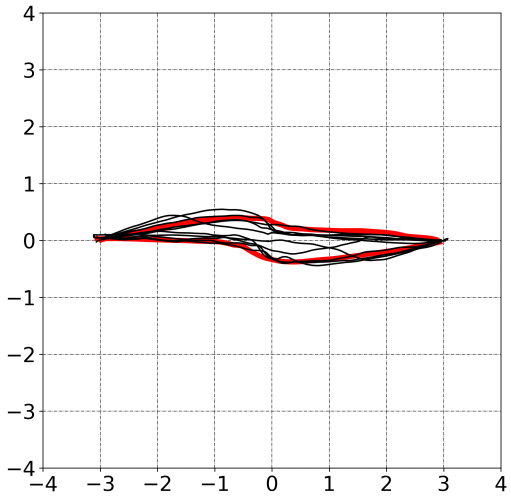

(a) Real Experiments

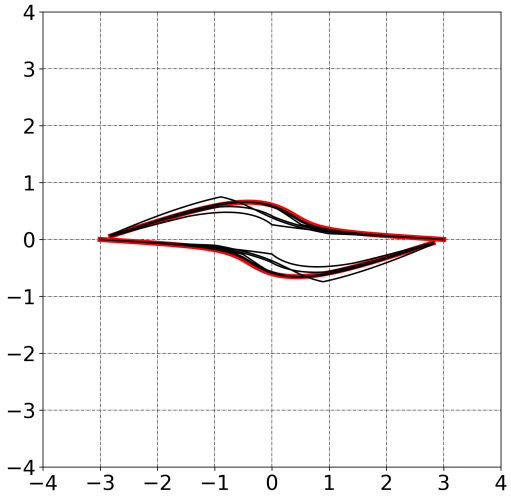

(b) Numerical Simulations

Fig. 12: Paths showing two drones swapping positions while avoiding each other using artificial potential fields. The first drone starts at (-3,0) and heads towards (3,0); the second drone starts at (3,0) and heads to (-3,0). This scenario is run multiple times while increasing the number of timesteps between positional updates n. These are incremented from $n = 1$ to $n = 160$ for $\Delta t = 0.025s$. As predicted, this has a significant effect on the paths of the drones. In (a) we see the paths for the real experiments in the flying arena. In (b) we see the paths for the numerical simulations of the same scenario. In both cases, the thick red line represents the lowest possible value of n, where drones are communicating the most.

- Both the theoretical predictions and the results from the numerical simulations were plotted together, showing a

promising correlation. However, to firmly establish this relationship, more data is necessary, which could entail more test cases or increasing the number of drones involved in the simulations.

- Beyond the simulations, real-world experiments were also conducted in our flying arena. The real drones used the same guidance algorithm (Artificial Potential Fields) as used in the simulations, and were instructed to swap positions in a simple scenario. The paths they followed in the process were recorded and compared with those from the simulations, providing a real-world validation of the developed theoretical framework.

Future research could focus on refining and testing the proposed framework with more complex scenarios or real-world drone operations. Furthermore, investigating the impact of other variables, such as drone speed, size, or onboard collision-avoidance systems, on the relationship between the number of drones and $n_{\max}$ could provide valuable insights.

Overall, the contributions made in this study, along with the empirical evidence and theoretical foundation, aim to enhance the safety and efficiency of drone operations in the progressively congested skies of the future.

REFERENCES

[1] Akshay Kumar Guruji, Himansh Agarwal, and D.K. Parsediya. Time-efficient a* algorithm for robot path planning. *Procedia Technology*, 23:144–149, 2016. 3rd International Conference on Innovations in Automation and Mechatronics Engineering 2016, ICIAME 2016 05-06 February, 2016.

[2] H. Wang, S. Lou, J. Jing, Y. Wang, W. Liu, and T. Liu. The ebs-a* algorithm: An improved a* algorithm for path planning. *PLoS ONE*, 17(2):e0263841, 2022.

[3] D. Xiang, H. Lin, J. Ouyang, and et al. Combined improved a* and greedy algorithm for path planning of multi-objective mobile robot. *Scientific Reports*, 12(13273), 2022.

[4] Jun Ding, Yinxuan Zhou, Xia Huang, Kun Song, Shiqing Lu, and Lusheng Wang. An improved rrt* algorithm for robot path planning based on path expansion heuristic sampling. *Journal of Computational Science*, 67:101937, 2023.

[5] Iram Noreen, Amna Khan, and Zulfiqar Habib. Optimal path planning using rrt* based approaches: A survey and future directions. *International Journal of Advanced Computer Science and Applications*, 7, 11 2016.

[6] Oussama Khatib. Real-time obstacle avoidance for manipulators and mobile robots. *The International Journal of Robotics Research*, 5(1):90–98, 1986.

[7] Iswanto Iswanto, Alfian Ma'arif, Oyas Wahyunggoro, and Adha Imam Cahyadi. Artificial potential field algorithm implementation for quadrotor path planning. *International Journal of Advanced Computer Science and Applications*, 10(8), 2019.

[8] Qidan Zhu, Yongjie Yan, and Zhuoyi Xing. Robot path planning based on artificial potential field approach with simulated annealing. In *Sixth International Conference on Intelligent Systems Design and Applications*, volume 2, pages 622–627, 2006.

[9] Guoqiang Hao, Qiang Lv, Zhen Huang, Huanlong Zhao, and Wei Chen. Uav path planning based on improved artificial potential field method. *Aerospace*, 10(6), 2023.

[10] Zeynep Bilgin, Murat Bronz, and Ilkay Yavrucuk. Panel Method Based Guidance for Fixed Wing Micro Aerial Vehicles. In *International Micro Air Vehicle Conference*, Delft, Netherlands, September 2022. TU-Delft.

[11] Han Liu. Linear strength vortex panel method for naca 4412 airfoil. *IOP Conference Series: Materials Science and Engineering*, 326:012016, 03 2018.

[12] Qiannan Cui, Peizhi Liu, Jinhua Wang, and Jing Yu. Brief analysis of drone swarms communication. In *2017 IEEE International Conference on Unmanned Systems (ICUS)*, pages 463–466, 2017.

[13] G. Asaamoning, P. Mendes, D. Rosário, and E. Cerqueira. Drone swarms as networked control systems by integration of networking and computing. *Sensors*, 21(8):2642, 2021.

[14] Xiaopan Zhu, Chun-Jiang Bian, Yu Chen, and Shi Chen. A low latency clustering method for large-scale drone swarms. *IEEE Access*, 7:186260–186267, 2019.

[15] MitchCampion, PrakashRanganathan, and SalehFaruque. Uav swarm communication and control architectures: a review. *Journal of Unmanned Vehicle Systems*, 7(2):93–106, 2018.

[16] Farrukh Javed, Humayun Zubair Khan, and Raheel Anjum. Communication capacity maximization in drone swarms. *Drone Systems and Applications*, 11:1–12, 2023.

[17] ICAO Annex 2 Rules of the Air. Chapter 3.2, avoidance of collisions, July 2005.

[18] P. Talwalkar. Distance between two random points in a square – sunday puzzle, July 3 2016.

[19] Saurabh Dasgupta. Surprising behaviour of the average nearest neighbour distance in a cluster of points. April 2 2021.